

THE FINE-GRAINED PARALLEL MICRO-GENETIC ALGORITHM AND ITS APPLICATION TO BROADBAND CONICAL CORRUGATED-HORN ANTENNA

Lei Chang¹, Hai-Jing Zhou², Ling-Lu Chen¹,
Xiang-Zheng Xiong¹, and Cheng Liao^{1, *}

¹Institute of Electromagnetics, Southwest Jiaotong University, Chengdu, Sichuan 610031, China

²Institute of Applied Physics and Computational Mathematics, Beijing 100094, China

Abstract—The fine-grained parallel micro-genetic algorithm (FGP-MGA) is developed to solve antenna design problems. The synthesis of uniformly excited unequally spaced array is presented. Comparison with the micro-genetic algorithm (MGA) has been carried out. It is seen that the FGPMGA significantly outperforms MGA, in terms of both the convergence rate and exploration ability. The FGPMGA can also reduce the optimization time. Then the FGPMGA and the body of revolution finite-difference time-domain (BOR-FDTD) are combined to achieve an automated design process for conical corrugated-horn antenna. Numerical simulation results show that the horn antenna has good impedance matching (the VSWR is less than 1.5), stable beamwidth and gain, as well as good rotation symmetry patterns over the whole band 8~13 GHz.

1. INTRODUCTION

In recent years, several evolutionary algorithms have emerged for solving design problems in electromagnetics such as genetic algorithm (GA) [1–5], micro-genetic algorithm (MGA) [6, 7], particle swarm optimization (PSO) [8–11] and differential evolution strategy (DES) [12–16].

GA is a popular global optimization algorithm. It is well known that one of the most attractive features of GA is the parallelism

Received 9 March 2013, Accepted 8 April 2013, Scheduled 11 April 2013

* Corresponding author: Cheng Liao (c.liao@home.swjtu.edu.cn).

that allows an effective search in the solution space. Several parallel techniques have been proposed to help maintain diversity in the population, and subsequently avoiding the premature convergence. In [17, 18], the parallel GAs in a master-slave model were proposed to design antenna arrays. In this parallel model, one population is used, but the evaluation of the fitness function are executed in parallel. So the behavior of the master-slave algorithm is essentially the same as a serial GA. The coarse-grained parallel GA was applied in [19, 20]. This parallel model divides a large population into some sub-populations, and independently performs selection, crossover and mutation on each subpopulation. A migration operator is used to send some individuals from one deme to another. The fine-grained model is also one of the most popular parallel techniques. In [21, 22], the fine-grained parallel GAs were used. Individuals of this model are usually placed on a large 2D grid. Fitness evaluation is done simultaneously for all individuals, selection, crossover and mutation take place within a local neighborhood. The coarse-grained and fine-grained models can accelerate the convergence rate and avoid the premature convergence.

The MGA is GA with a small population size which can speed up the converge, and has been applied to antenna [6] and power divider [7] design problems. In [23], the master-slave parallel MGA was used to optimize a frequency selective surface (FSS). The coarse-grained parallel MGA (CGPMGA) was applied to solve ultra-wideband power divider problem [24] and tune power system stabilizer in multimachine power system [25]. At present, the fine-grained Parallel MGA (FGPMGA) has not been applied to microwave engineering design problems. This work focuses on the analysis of the FGPMGA to improve the performance of classical MGA.

The BOR-FDTD employs a 2D solution problem instead of a full 3D one due to the axial symmetric property and saves computational resources [26–28]. This method is a robust and versatile numerical tool for solving axial symmetric problems. In [29], several smooth-walled axis-symmetrical dielectric-loaded horn antennas were optimized based on the BOR-FDTD technique and GA. Corrugated-conical horn antennas are commonly used in reflector antenna systems [30, 31], and the design of these systems requires the performance of the horns be very well. In this paper, the BOR-FDTD is used here to simulate a broadband conical corrugated-horn antenna, and the FGPMGA based on binary coding is applied to optimize the structure of the horn. The horn has an impedance bandwidth between 8~13 GHz with VSWR ≤ 1.5 , stable beamwidth and gain, as well as good circular symmetry patterns over this band.

This paper is organized as follows. Section 2 describes the

FGPMGA, an antenna array pattern synthesis is provided to demonstrate the advantages of our algorithm. In Section 3 a dual-mode conical horn antenna is simulated using BOR-FDTD and CST Microwave Studio. The correctness of BOR-FDTD is verified. In Section 4, the combined method between the FGPMGA and the BOR-FDTD is used to optimize the corrugated-conical horn antenna, in addition, the numerical results are presented. Conclusions are given in Section 5.

2. THE FINE-GRAINED PARALLEL MICRO-GENETIC ALGORITHM

The fine-grained parallel model is also called neighborhood model. Each processor is allocated only one individual and selects parents for recombination from local neighborhood by considering neighbors at different distances. For the FGPMGA, a 4- n neighborhood is used, as shown in Figure 1. In this case each node represents a single individual. The FGPMGA is implemented using C++ on a message passing interface (MPI) environment.

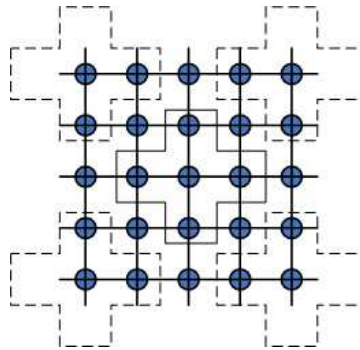


Figure 1. The FGPMGA architecture.

In each neighborhood, different crossover and mutation probability, as well as different methods of mutation and crossover. The procedure of the FGPMGA is as follows.

We carry out a linear array synthesis to demonstrate the superior of the FGPMGA. A 32-element uniformly excited linear array is considered, which symmetrically placed along the x -axis. The position-only method is used to reduce the side-lobe level (SLL). Only half of the optimization parameters $\{x_1, \dots, x_{16}\}$ are considered. The array

Algorithm 1 Pseudo code for the FGPMGA

Initialization:

```

1:  $G \leftarrow 1$ ;
2: for each node do
3:   initialize an individual randomly in parallel;
4:   calculate fitness values;
5: end for

```

Iteration:

```

6: while termination conditions not met do
7:   Create MPI Cartesian process topology;
8:   for each node do
9:     set crossover and mutation rate;
10:    set methods of mutation and crossover;
11:    select an individual randomly from neighborhood;
12:    crossover with the local individual;
13:    mutate individual according to mutation rate;
14:    calculate fitness values of new individual, and update
       individual if new one is better;
15:   end for
16:   save the best individual;
17:   if  $\text{mod}(G, G_{\text{refresh}}) = 0$  then
18:     keep the best individual and initialize the others;
19:   end if
20:    $G \leftarrow G + 1$ ;
21: end while

```

factor can be written as

$$AF(\theta, \bar{x}) = 2 \sum_{i=1}^{16} \left(\cos \left(\frac{2\pi}{\lambda} x_i \sin \theta \right) \right). \quad (1)$$

The angle resolution of θ is 0.1° . We assume that $d_{\min} = 0.5\lambda \leq x_i - x_{i-1} \leq d_{\max} = 0.6\lambda$. The population size is set as 100. There are 100 parallel processes in the FGPMGA. The total number of iterations is set to 2000. Figure 2 shows the average convergence rates for FGPMGA, CGPMGA [24] (10 sub-populations) and MGA in 5 independent runs. It is obvious that FGPMGA converges faster than CGPMGA and MGA. The FGPMGA and CGPMGA converge to the same best value (-15.82 dB) that agrees with the results obtained by modified DES in [13, 16]. However, the SLL obtained by the MGA is only -15.81 dB. The average number of iterations of FGPMGA is 242 evaluations, while 816 iterations are needed for the CGPMGA. Furthermore, the FGPMGA only needs 242 evaluations

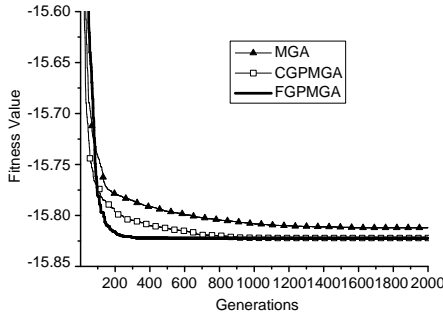


Figure 2. Comparisons of the average convergence rates for FGPMGA, MGA, CGPMGA and MGA.

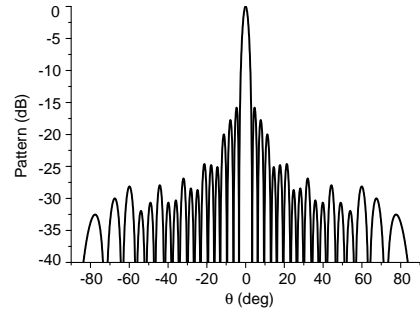


Figure 3. Radiation pattern for a 32-element uniform amplitude array.

on each processor in contrast to 8160 evaluations by the CGPMGA. Figure 3 shows the optimal pattern obtained by the FGPMGA.

3. THE BODY OF REVOLUTION FINITE-DIFFERENCE TIME-DOMAIN

The BOR-FDTD reduces the original 3D Maxwell's equation to a 2D form. The termination of the computational domain uses the perfectly matched layer (PML) absorbing boundary conditions [26]. The excitation is introduced in a cross-section, by setting the corresponding components of the fields to vary in time as a modulated Gaussian pulse [27]. A fast near-to-far-field transformation method proposed in [28] is used.

We simulate a dual-mode conical horn antenna to validate the BOR-FDTD program, as shown in Figure 4. The horn is excited by using a TE_{11} mode. The source excitation function used for this work is

$$g(t) = \cos(2\pi f_0 t) \exp\left[-\frac{4\pi(t-t_0)^2}{\tau^2}\right] \quad (2)$$

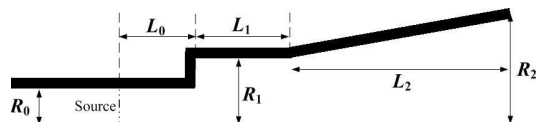


Figure 4. Dual-mode conical horn antenna.

where, $\tau = 2/1.5 \times 10^{-9}$ ns, $t_0 = 0.9\tau$, $f_0 = 2.0$ GHz. The parameters of the horn are as follows: $L_0 = 16$ mm, $R_0 = 17.1$ mm, $L_1 = 22$ mm, $R_1 = 22.7$ mm, $L_2 = 149.8$ mm, $R_2 = 45$ mm.

Figure 5 gives the distribution of near-field E_r at different time step. Figure 6 shows the far-field patterns in the E -plane and H -plane, and compares it with those obtained by using the CST Microwave Studio. It is shown that the two trends are very similar.

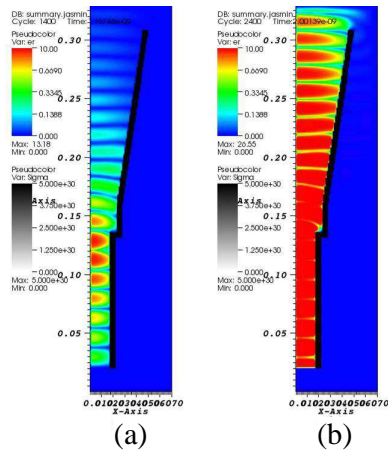


Figure 5. The distribution of E_r at different moments. (a) 1400 time-step. (b) 2400 time-step.

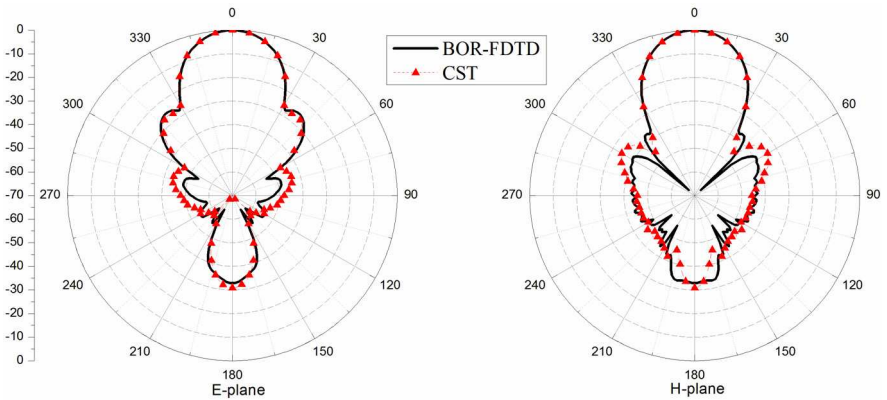


Figure 6. Radiation patterns.

4. RESULTS OF CORRUGATED-CONICAL HORN ANTENNA OPTIMIZATION

A corrugated-conical horn antenna with horizontal corrugations (see Figure 7) is optimized by the combined methods between FGPMGA and BOR-FDTD. The radius and length of the input waveguide is $R_0 = 13.6$ mm and $L_0 = 20$ mm, respectively. The thickness of metal is 2 mm. The antenna is also excited with a TE_{11} mode between 8 and 13 GHz. The source function is shown in Eq. (2), where $\tau = 2/2.5 \times 10^{-9}$ ns, $t_0 = 0.9\tau$, $f_0 = 10.5$ GHz. The semi-flare angle of horn is α . The depth and height of the corrugations is L_1 and R_a , respectively. The parameter L_d can be calculated as follows:

$$L_d = R_a / \tan \alpha$$

(3)

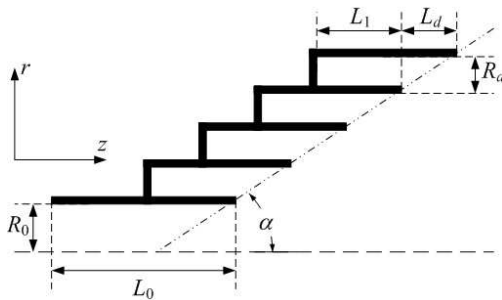


Figure 7. Geometry of the corrugated-conical horn antenna.

The size of corrugations has effects on the satisfaction of the balanced hybrid-mode condition. In order to establish the balanced HE_{11} mode at the horn aperture, the parameters of α , L_1 and R_a are optimized. Their ranges are listed in Table 1.

The horn is designed with equal E and H patterns between -53° and 53° . Besides, the edge power level is -15 dB. The design problem

Table 1. Design parameters for the horn.

	α	L_1	R_a
Lower bounds	10°	2 mm	3 mm
Upper bounds	60°	16 mm	10 mm

is defined as the minimization of the objective function:

$$\text{fitness} = \min \sum_{i=1}^3 \left\{ \sum_{0 \leq \theta \leq 53^\circ} [a_i |F_E(f_i, \theta) - F_H(f_i, \theta)|_{\text{dB}}] + b_i |F_E(f_i, 53^\circ) + 15|_{\text{dB}} \right\} \quad (4)$$

where, $i = 1, 2, 3$; $f_{i=1,2,3} = \{8 \text{ GHz}, 10.5 \text{ GHz}, 13 \text{ GHz}\}$; a_i and b_i are the weight factors of the i -th frequency: $a_1 + b_1 = a_3 + b_3 = 4$, $a_2 + b_2 = 10$, and $a_1 = a_3 = 3$, $a_2 = 7$. The population size is set to 30 and the total number of iterations set to 100. 30 processors on the SUGON TC2600 blade server are used for computing. It is worth noting that the calculation time of the optimization is dominated by the number of BOR-FDTD computation on each processor. The optimal parameters obtained by the FGPMGA are as follows: $\alpha = 40^\circ$, $L_1 = 8 \text{ mm}$, $R_a = 5 \text{ mm}$. The normalized radiation patterns in the E

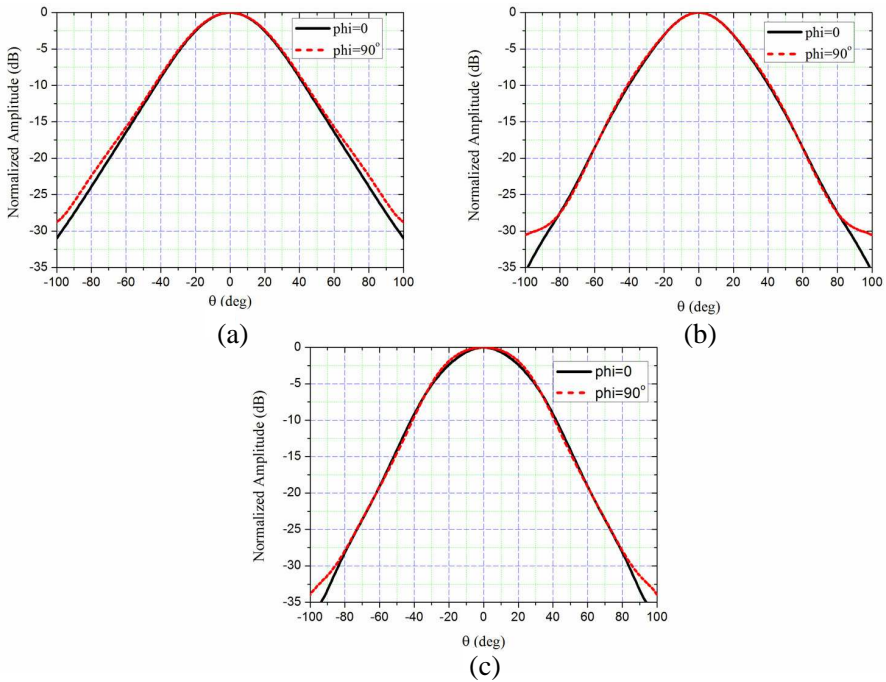


Figure 8. The normalized radiation patterns of the three frequencies. (a) 8 GHz. (b) 10.5 GHz. (c) 13 GHz.

and H planes at 8, 10.5 and 13 GHz based on the optimal parameters are presented in Figure 8.

It can be seen that the horn antenna has good rotation symmetry in the radiation patterns. Table 2 shows the edge power level of the principal planes at $\theta = 53^\circ$. The E and H patterns are equal in the illuminated area ($-53^\circ \leq \theta \leq 53^\circ$).

Figure 9 presents the VSWR of the horn. Over the frequency range of 8 to 13 GHz, the VSWR is less than 1.5. The gain of the antenna is shown in Figure 10. The variation range of gain is from 12.14 dBi to 13.07 dBi. The half-power beamwidths as a function of frequency of the antenna in the principal planes are depicted in Figure 11. It is shown that the half-power beamwidths in the E and H planes have a maximum difference of 5.57° . The optimization time for corrugated-conical horn antenna is 6375 seconds and about equal to that of the

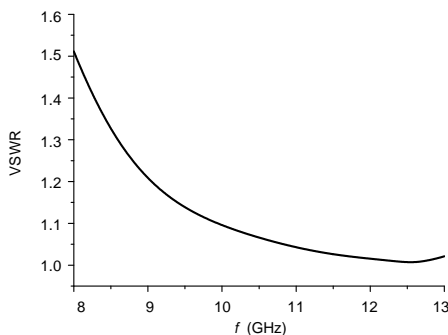


Figure 9. The VSWR of the corrugated-conical horn antenna.

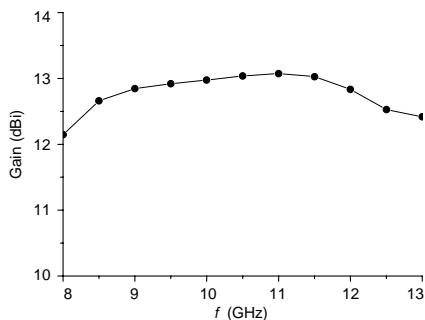


Figure 10. The simulated gain of the corrugated-conical horn antenna.

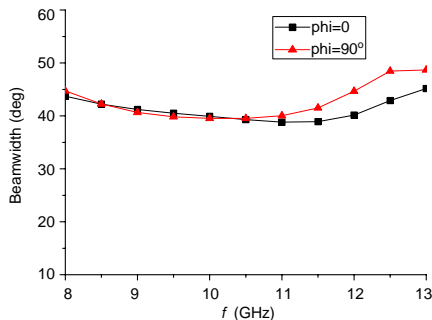


Figure 11. A comparison of the half-power beamwidths in the principal planes.

Table 2. The relative level of the principal planes (unit: dB).

	$\varphi = 0$	$\varphi = 90^\circ$
$f = 8 \text{ GHz}$	-14.05	-13.93
$f = 10.5 \text{ GHz}$	-15.23	-15.31
$f = 13 \text{ GHz}$	-15.60	-15.96

horn simulated by the BOR-FDTD for 100 times. However, MGA needs 3000 times calculation using the BOR-FDTD.

5. CONCLUSION

In this paper, a fine-grained parallel micro-genetic algorithm has been introduced. Each processor is allocated only one individual. The proposed technique has been applied to linear array synthesis by position-only control. The results show that the FGPMGA performs much better than the classical MGA and the CGPMGA in obtaining the optimum pattern with minimum number of the object function evaluations. Besides, A corrugated-conical horn antenna with horizontal corrugations was optimized using the BOR-FDTD/FGPMGA method. Across the 8~13 GHz band, the horn antenna exhibits good performance. The VSWR is less than 1.5. The patterns of E and H planes are equal, and have good rotation symmetry. The stable beamwidth and gain are also achieved. It can be concluded that the proposed algorithm is expected to be an applicable optimization tool for other electromagnetic problems.

ACKNOWLEDGMENT

This work was supported by the National Basic Research Program of China (973 Program, Grant No. 2013CB328904), the NSAF of China (Grant No. 11076022), and the Research Fund of Key Laboratory of CEMC Science & Technology of CAEP (FZ2012-2-01).

REFERENCES

1. Wang, R., J. Xu, C. L. Wei, M. Y. Wang, and X. C. Zhang, "Improved extraction of coupling matrix and unloaded Q from S -parameters of lossy resonator filters," *Progress In Electromagnetics Research*, Vol. 120, 67–81, 2011.

2. Jian, L., G. Xu, J. Song, H. Xue, D. Zhao, and J. Liang, "Optimum design for improving modulating-effect of coaxial magnetic gear using response surface methodology and genetic algorithm," *Progress In Electromagnetics Research*, Vol. 116, 297–312, 2011.
3. Zhu, X., W. Shao, J. L. Li, and Y. Dong, "Design and optimization of low RCS patch antennas based on a genetic algorithm," *Progress In Electromagnetics Research*, Vol. 122, 327–339, 2012.
4. Yu, X. H., L. Wang, H. G. Wang, X. D. Wu, and Y. H. Shang, "A novel multiport matching method for maximum capacity of an indoor mimo system," *Progress In Electromagnetics Research*, Vol. 130, 67–84, 2012.
5. Dai, G. L. and M. Y. Xia, "Design and optimization of a compact wideband hat-fed reflector antenna for satellite communications," *IEEE Transactions on Antennas and Propagation*, Vol. 61, No. 1, 125–133, 2013.
6. Watanabe, Y., K. Watanabe, and H. Igarashi, "Optimization of meander line antenna considering coupling between nonlinear circuit and electromagnetic waves for UHF-band RFID," *IEEE Transactions on Magnetics*, Vol. 47, No. 5, 1506–1509, 2011.
7. Wang, H., X. Tang, Y. Liu, and Y. Cao, "Analysis and design of ultra-wideband power divider by micro-genetic algorithm," *Journal of Electromagnetic Waves and Applications*, Vol. 26, No. 10, 1341–1349, 2012.
8. Lizzi, L., G. Oliveri, and A. Massa, "A time-domain approach to the synthesis of UWB antenna systems," *Progress In Electromagnetics Research*, Vol. 122, 557–575, 2012.
9. Weng, W. C. and C. L. Hung, "Design and optimization of a logo-type antenna for multiband applications," *Progress In Electromagnetics Research*, Vol. 123, 159–174, 2012.
10. Liu, D., Q. Y. Feng, W. B. Wang, and X. Yu, "Synthesis of unequally spaced antenna arrays by using inheritance learning particle swarm optimization," *Progress In Electromagnetics Research*, Vol. 118, 205–221, 2011.
11. Zaharis, Z. D., K. A. Gotsis, and J. N. Sahalos, "Adaptive beamforming with low side lobe level using neural networks trained by mutated boolean PSO," *Progress In Electromagnetics Research*, Vol. 127, 139–154, 2012.
12. Mallipeddi, R., J. P. Lie, P. N. Suganthan, S. G. Razul, and C. M. S. See, "A differential evolution approach for robust adaptive beamforming based on joint estimation of look direction and array geometry," *Progress In Electromagnetics Research*,

- Vol. 119, 381–394, 2011.
13. Chang, L., C. Liao, W. B. Lin, L. L. Chen, and X. Zheng, “A hybrid method based on differential evolution and continuous ant colony optimization and its application on wideband antenna design,” *Progress In Electromagnetics Research*, Vol. 122, 105–118, 2012.
 14. Mandal, A., H. Zafar, S. Das, and A. Vasilakos, “A modified differential evolution algorithm for shaped beam linear array antenna design,” *Progress In Electromagnetics Research*, Vol. 125, 439–457, 2012.
 15. Rocca, P., G. Oliveri, and A. Massa, “Differential evolution as applied to electromagnetics,” *IEEE Antennas and Propagation Magazine*, Vol. 53, No. 1, 38–49, 2011.
 16. Goudos, S. K., K. Siakavara, T. Samaras, E. E. Vafiadis, and J. N. Sahalos, “Self-adaptive differential evolution applied to real-valued antenna and microwave design problems,” *IEEE Transactions on Antennas and Propagation*, Vol. 59, No. 4, 1286–1298, 2011.
 17. Chen, X., G. S. Wang, and K. Huang, “A novel wideband and compact microstrip grid array antenna,” *IEEE Transactions on Antennas and Propagation*, Vol. 58, No. 2, 596–599, 2010.
 18. Wang, G. S., S. Y. Lin, W. D. Fang, and W. X. Zhang, “Design of a compact wideband high-gain microstrip grid array antenna,” *Microwave and Optical Technology Letters*, Vol. 53, No. 5, 1144–1147, 2011.
 19. Tsai, C. C., H. C. Huang, and C. K. Chan, “Parallel elite genetic algorithm and its application to global path planning for autonomous robot navigation,” *IEEE Transactions on Industrial Electronics*, Vol. 58, No. 10, 4813–4821, 2011.
 20. Rodriguez, M., D. M. Escalante, and A. Peregrin, “Efficient distributed genetic algorithm for rule extraction,” *Applied Soft Computing*, Vol. 11, No. 1, 733–743, 2011.
 21. Georgoudas, I. G., G. C. Sirakoulis, E. M. Scordilis, and I. Andreadis, “Parametric optimisation in a 2-D cellular automata model of fundamental seismic attributes with the use of genetic algorithms,” *Advances in Engineering Software*, Vol. 42, No. 9, 623–633, 2011.
 22. Horvath, A. and M. Rasonyi, “Implementation of cellular genetic algorithms on a CNN chip: Simulations and experimental results,” *International Journal of Circuit Theory and Applications*, Vol. 40, No. 12, 1321–1332, 2012.

23. Chakravarty, S. and R. Mittra, "Design of a frequency selective surface (FSS) with very low cross-polarization discrimination via the parallel micro-genetic algorithm (PMGA)," *IEEE Transactions on Antennas and Propagation*, Vol. 51, No. 7, 596–599, 2003.
24. Chang, L., C. Liao, L. L. Chen, W. B. Lin, X. Zheng, and Y. L. Wu, "Design of an ultra-wideband power divider via the coarse-grained parallel micro-genetic algorithm," *Progress In Electromagnetics Research*, Vol. 124, 425–440, 2012.
25. Hongesombut, K., Y. Mitani, S. Dechanupaprittha, I. Ngamroo, K. Pasupa, and J. Tippayachai, "Power system stabilizer tuning based on multiobjective design using hierarchical and parallel micro genetic algorithm," *POWERCON 2004 — International Conference on Power System Technology*, 402–407, Singapore, 2004.
26. Liu, Y. L., Z. W. Lu, Z. B. Ren, F. Y. Li, and Z. L. Cao, "Perfectly matched layer absorbing boundary conditions in rigorous vector analysis of axially symmetric diffractive optical elements," *Optics Communications*, Vol. 223, No. 1–3, 39–45, 2003.
27. Tong, M. S., R. Sauleau, A. Rolland, and T. G. Chang, "Analysis of electromagnetic band-gap waveguide structures using body-of-revolution finite-difference time-domain method," *Microwave and Optical Technology Letters*, Vol. 49, No. 9, 2201–2206, 2007.
28. Farahat, N., W. H. Yu, and R. Mittra, "A fast near-to-far-field transformation in body of revolution finite-difference time-domain method," *IEEE Transactions on Antennas and Propagation*, Vol. 51, No. 9, 2534–2540, 2003.
29. Rolland, A., N. T. Nguyen, R. Sauleau, C. Person, and L. Le Coq, "Smooth-walled light-weight Ka-band shaped horn antennas in metallized foam," *IEEE Transactions on Antennas and Propagation*, Vol. 60, No. 3, 1245–1251, 2012.
30. Teniente, J., R. Gonzalo, and C. del Rio, "Low sidelobe corrugated horn antennas for radio telescopes to maximize G/T-s," *IEEE Transactions on Antennas and Propagation*, Vol. 59, No. 6, 1886–1893, 2011.
31. Zhang, T. L., Z. H. Yan, F. F. Fan, and B. Li, "Solving job shop scheduling problem using a hybrid parallel micro genetic algorithm," *Journal of Electromagnetic Waves and Applications*, Vol. 25, No. 1, 123–129, 2011.